Supporting Information

An investigation into the factors governing the oxidation of two-dimensional Ti_3C_2 MXene.

Yoonjeong Chae,[a,] *Seon Joon Kim,*[b,c] *Soo-Yeon Cho,*[d,e] *Junghoon Choi,* [d,e] *Kathleen Maleski,*[f] *Byeong-Joo Lee,* [a] *Hee-Tae Jung,* [d,e] *Yury Gogotsi,*[f] *Yonghee Lee,* [*,a] *and Chi Won Ahn*[*,a]

[a] Global Nanotechnology Development Team, National Nano Fab Center (NNFC), Daejeon 34141, South Korea

[b] Department of Materials Science and Engineering, and A.J. Drexel Nanomaterials Institute, Drexel University, Philadelphia, PA 19104, USA

[c] Wearable Platform Materials Technology Center, Korea Advanced Institute of Science and Technology (KAIST), Daejeon 34141, South Korea

[d] Department of Chemical and Biomolecular Engineering (BK-21 Plus), Korea Advanced Institute of Science and Technology (KAIST), Daejeon 34141, South Korea

[e] KAIST Institute for the NanoCentury, Daejeon 34141, South Korea

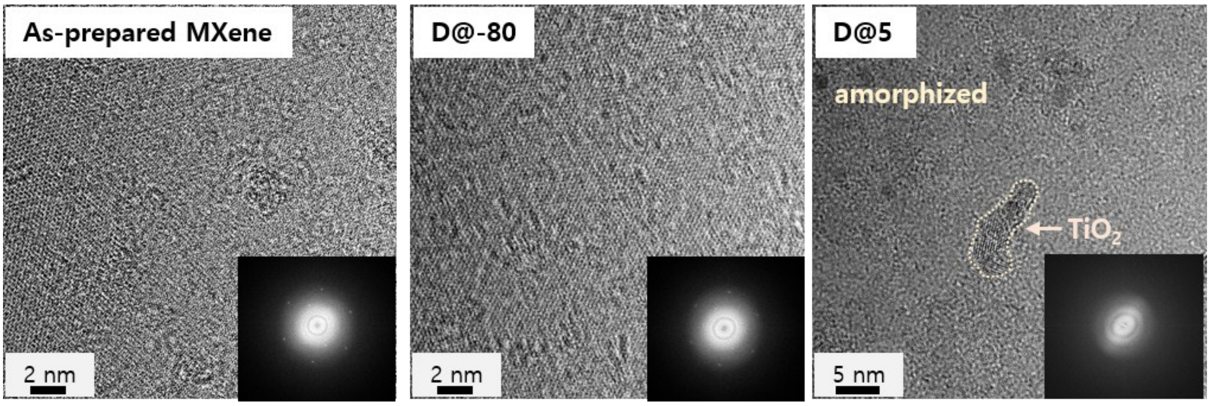

Figure S1. TEM images of as-synthesized MXene, D@-80 and D@5.

Individual atomic structures that are not oxidized can be seen on MXene sheet made from as-prepared solution and from D@-80. A TEM image of the MXene sheet stored at D@5 shows that some of MXene sheets were already oxidized (TiO_2), and they are amorphized, which would make it significantly easier for the structure to decompose further into TiO_2.

FFT alignment is clearly shown in the as-synthesized solution indicating the presence of MXene, but is not shown in the D@5 solution (5 weeks of storage).

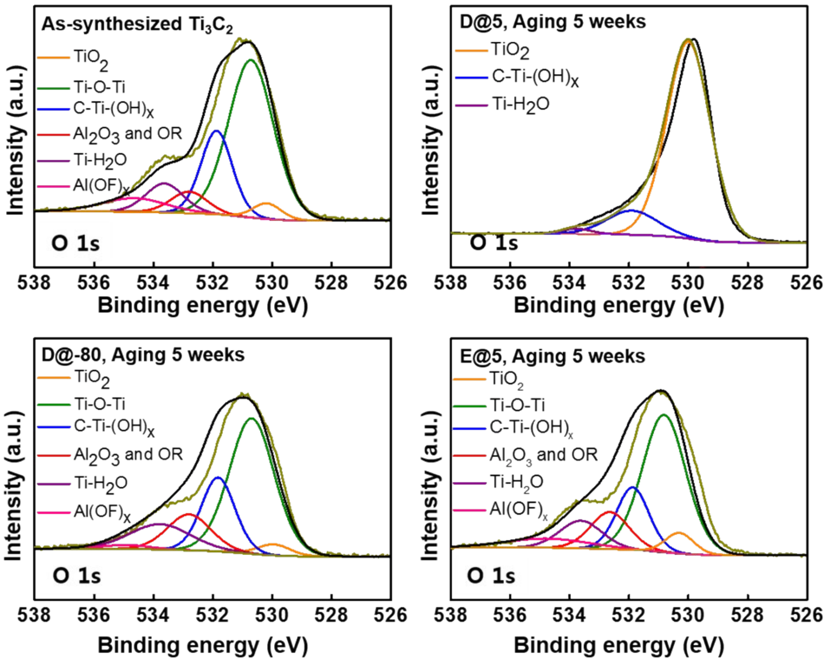

Assigned to	As-synthesized Ti_3C_2		Aging 5 weeks@5℃	
	BE (eV)	Fraction (%)	BE (eV)	Fraction (%)
TiO_2	530.1	3.3	530	86.2
Ti-O-Ti	530.7	55.2		
C-Ti-$(OH)_x$	531.8	20.4	531.9	12.1
Al_2O_3 and OR	532.8	6.1		
Ti-H_2O	533.6	8.3	533.7	1.7
$Al(OF)_x$	534.6	6.6		

Figure S2. X-ray photoelectron spectra samples (as-synthesized, aged for 5 weeks at D@5, aged for 5 weeks at D@-80, and aged for 5 weeks at E@5) with deconvoluted components at O 1s. [1-6]

The $Ti_3C_2T_x$ solutions stored for 5 weeks were examined with XPS to assess changes in the surface chemistry during aging. The XPS data show that the freshly prepared $Ti_3C_2T_x$ barely shows TiO_2 peak, but the $Ti_3C_2T_x$ solution stored at 5°C produces a remarkable TiO_2 peak due to oxidation. C-Ti-$(OH)_x$ decreased from 20.4% to 12.1%, while atomic weight of TiO_2

increased from 3.3% to 86.2%.

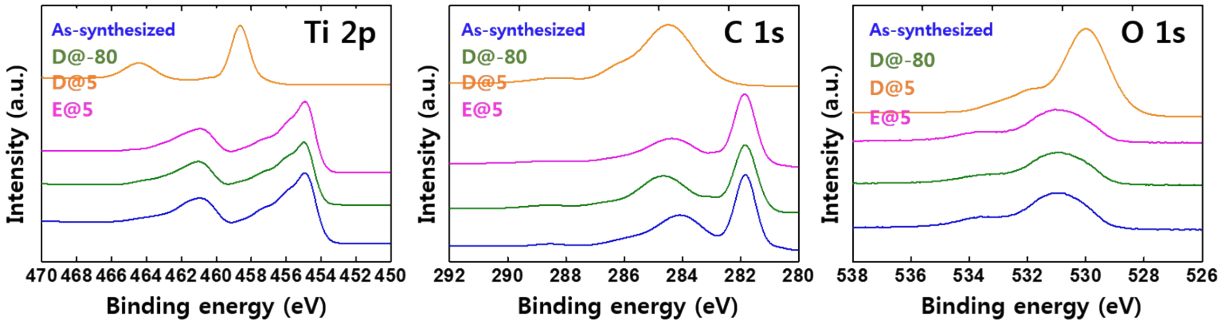

Figure S3. XPS measurements revealing the temperature dependent behavior of Ti 2p, C 1s and O 1s.

Under each storage condition, As-synthesized, D@-80 and E@5 show similar shapes. In Ti 2p, two peaks of (a) and (b) are shown, and it is confirmed that the TiO_2 peaks appear strongly as they are oxidized. In C 1s, the peak of Ti-C almost disappeared, and the peak of C-C remarkably increased. Finally, in O 1s, Ti-O-Ti bonds around 530.7 eV are reduced and TiO_2 peaks of 530.1 eV are observed. [7]

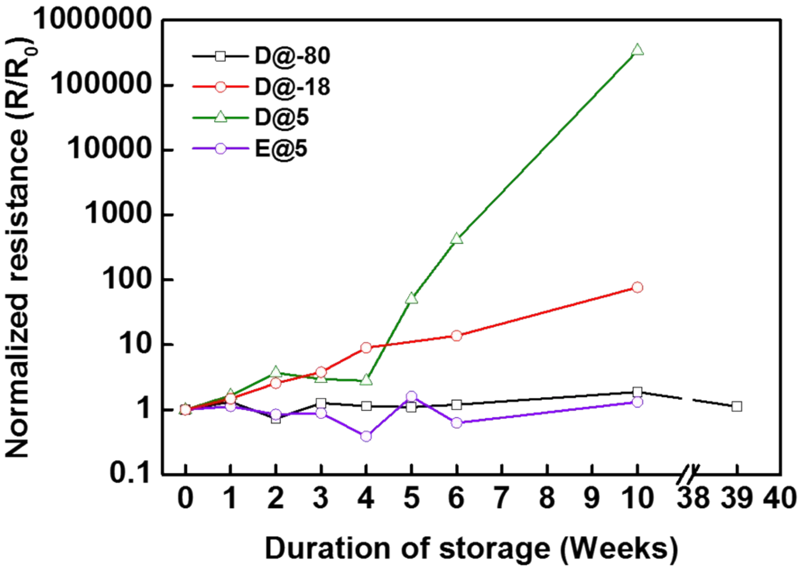

Figure S4. The normalized sheet resistances of Ti_3C_2 MXene films prepared from solutions stored under various conditions for up to 40 weeks.

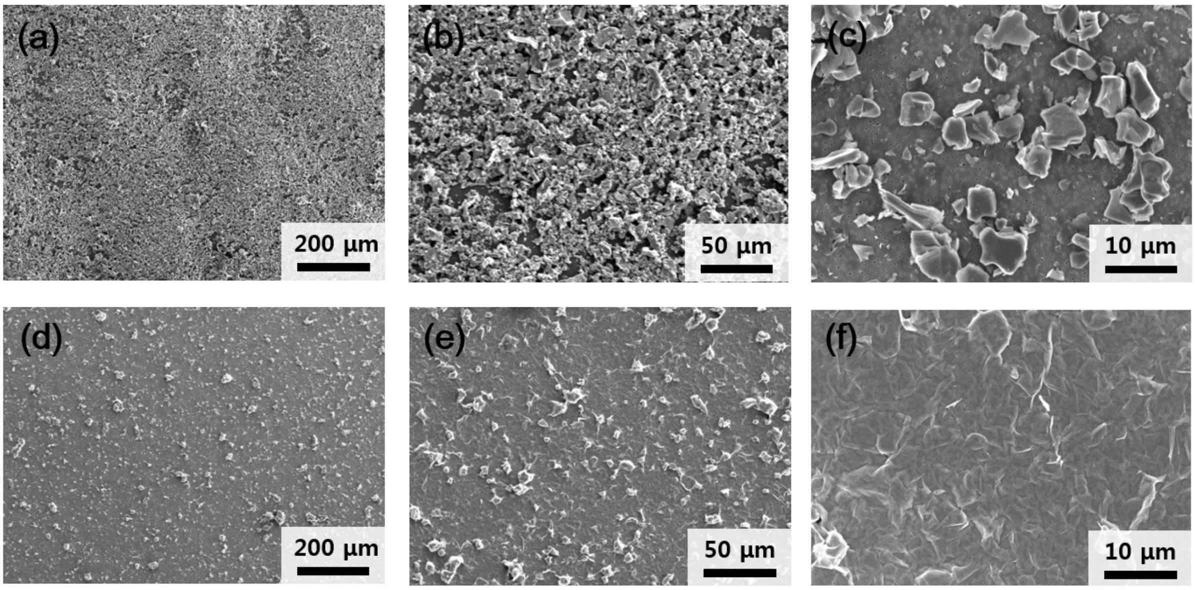

Figure S5. These SEM images of Ti_3C_2 MXene films at various magnifications. SEM images of vacuum filtered film of Ti_3C_2 dispersed in ethanol at 5°C are shown in (a), (b), and (c). SEM images of vacuum filtered film of Ti_3C_2 re-dispersed in DI water are shown in (d), (e), and (f).

The dispersion of Ti_3C_2 MXene in an organic solvent results in the aggregation of particles as shown in (a), (b) and (c). However, the MXene solution dispersed in ethanol was centrifuged at 5000 rpm, ethanol solution was discarded, and DI water was added into the centrifugation bottle to disperse again. The Ti_3C_2 flakes are well-dispersed as shown in (d), (e) and (f).

The dispersions in the non-aqueous organic solvent (ethanol) were stored at -80°C, -18°C, and 5°C. We used a representative organic solvent, ethanol. However, $Ti_3C_2T_x$ does not disperse as well in ethanol compared to dispersions in water: some of the $Ti_3C_2T_x$ particles are aggregated and sediment to the bottom of the tube. Furthermore because of the aggregation, the $Ti_3C_2T_x$ flakes dispersed in ethanol do not exhibit a good free-standing film. To solve this problem, a dispersion of $Ti_3C_2T_x$ in an anhydrous organic solvent was re-dispersed in DI water by using centrifugation, and then the re-dispersed solution (in DI water) was used to prepare a film through vacuum filtration.

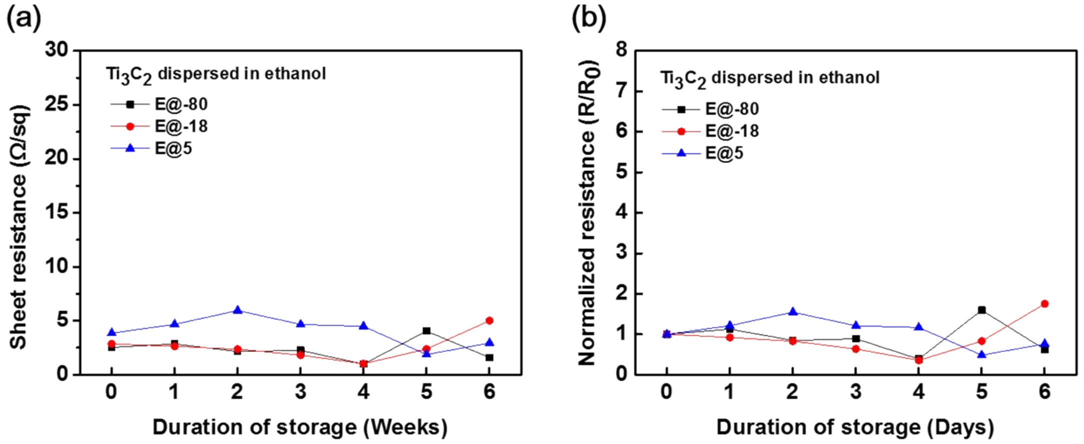

Figure S6. (a) Sheet resistances of Ti_3C_2 MXene films prepared from dispersions in anhydrous organic solvent aged for 6 weeks at various temperatures. (b) Normalized values of the sheet resistances of Ti_3C_2 MXene films prepared from dispersions in an anhydrous organic solvent.

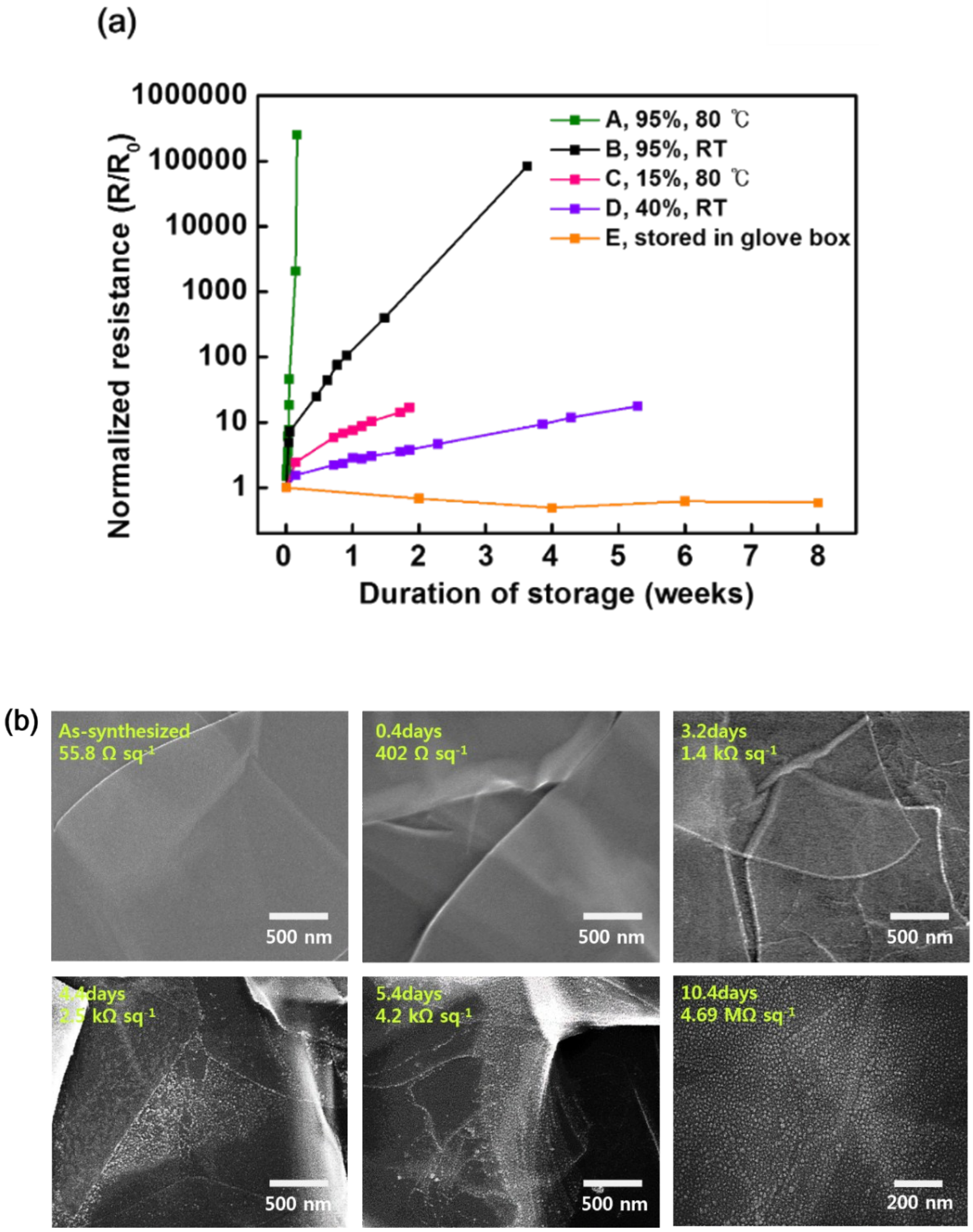

Figure S7. (a) Normalized resistances of various $Ti_3C_2T_x$ MXene films obtained with vacuum filtration after storage for up to 8 weeks at various temperatures and humidity. (b) Sequential SEM images of film B, which was stored at the room temperature (25°C) and a humidity of 95%.

As appears in **Figure S7a**, even if the samples were stored at the same temperature, the oxidation proceeds more rapidly if the humidity conditions are different. We have demonstrated that the oxidation of $Ti_3C_2T_x$ is affected by moisture in the air, and the amount of exposure to air changes the electrical conductivity of the MXene film. This has implications for the storage of $Ti_3C_2T_x$ films, and suggests that $Ti_3C_2T_x$ may be oxidized to differing degrees depending on the season. **Figure S7b** shows the microstructure of oxidized $Ti_3C_2T_x$. In the fresh state, no TiO_2 is visible, but TiO_2 gradually forms as oxidation proceeds. TiO_2 begins to form through oxidation at the edges of the flake, and eventually completely covers the surface.

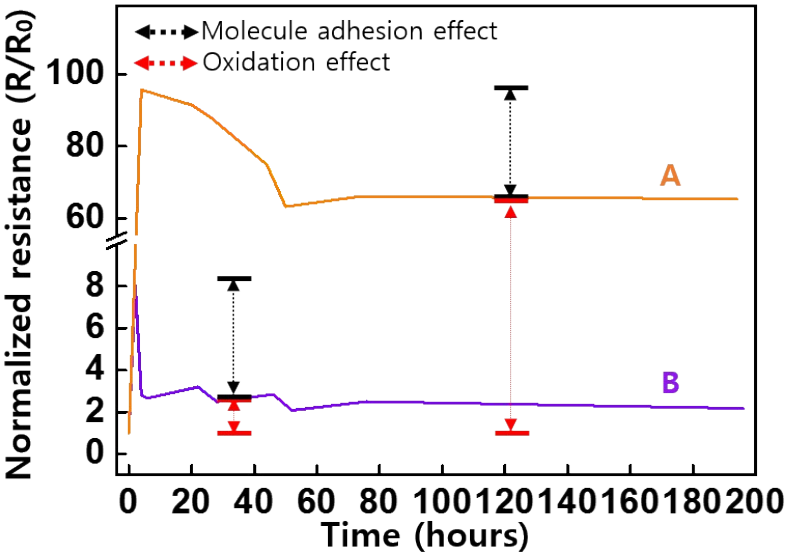

	Molecular adhesion effect (change in sheet resistance)	Oxidation effect (change in sheet resistance)
100-fold increase (Sample **A**)	About 40% (100 to 60)	About 60% (60 to 1)
10-fold increase (Sample **B**)	About 75% (8 to 2)	About 25% (2 to 1)

Figure S8. Experiments on the change of sheet resistance of the film to examine the adhesion effect of water and gas molecules.

Experimental methods

a) Keep two MXene films at 80°C and humidity of 95% condition.

b) Keep the one sample until sheet resistance increases 10 times. Also, keep the other one sample until sheet resistance increase 100 times. (100-fold increase in sample: **A**, 10-fold increase in sample: **B**)

c) After the sheet resistance of the sample reaches the reference value, the sample is held in a vacuum state in a desiccator (for vacuum annealing) and changes of sheet resistance are shown as follows.

The sheet resistance ratio of **Sample A** decreased by 40% and that of **Sample B** by 75% due to the molecular adhesion effect. In addition, due to the oxidation effect, the sheet resistance ratio decreased by 75% and the sample b by 25%.

The increase of sheet resistance does not necessarily mean oxidation. (In film D (**Figure S7**), even if the sheet resistance of the film increases steadily, this phenomenon may be possible due to the adherence of water and gas molecules from the ambient to the MXene film.8)To investigate, we oxidized the film on purpose and examined the change of sheet resistance after the vacuum annealing. As a result, the increased resistance dropped to a certain level again, and then remained saturated. This result appears to have increased temporarily by water and gas molecules and the saturated range is predicted to be completely oxidized. Thus, various analysis such as EDS, Raman, and SEM are required to investigate the oxidation. We showed the oxidation process of MXene through various analysis.

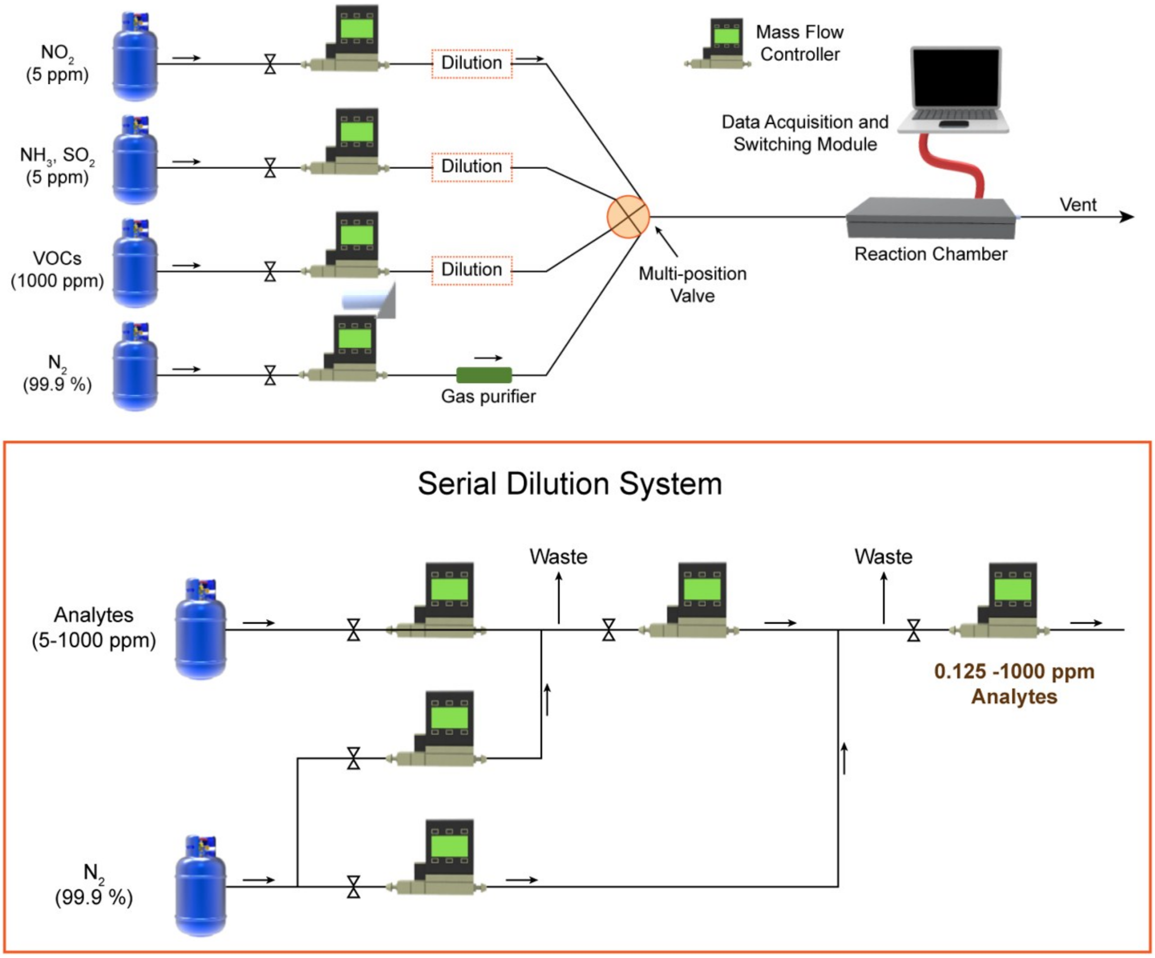

Figure S9. Schematic diagram of the gas delivery system. Various analytes and N_2 are introduced in a controlled manner into the reaction chamber by using the MFC, the tubing system, and multi-position valves. A serial dilution system was also used to obtain concentrations of the analyzed gas in the range 2.5–30000 ppm.

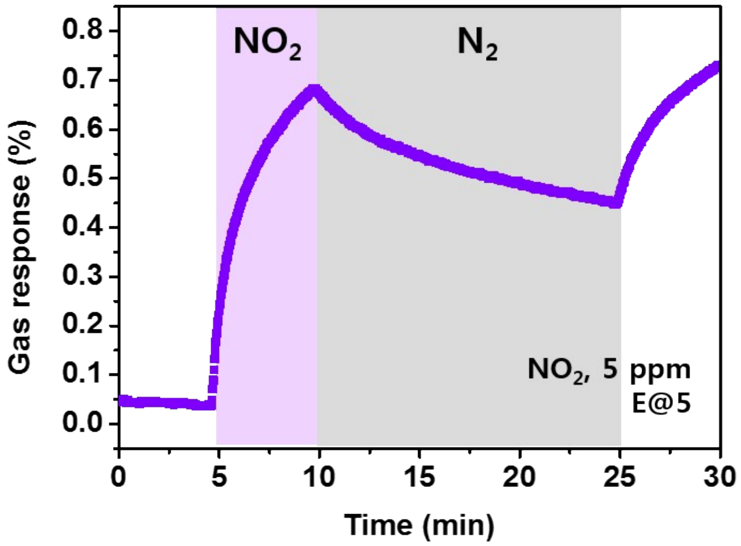

Figure S10. Gas sensor responses of films prepared from $Ti_3C_2T_x$ solutions aged in an anhydrous organic solvent for 5 weeks. The gas response of the MXene stored in the organic solvent toward 5 ppm NO_2 is approximately 0.63%.

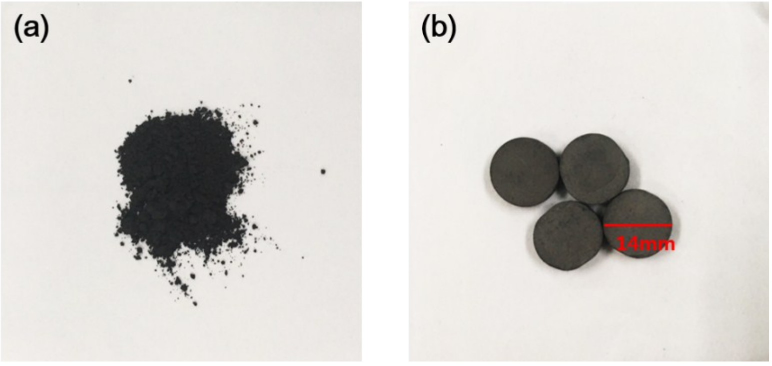

Figure S11. Photographs of (a) 2 g Ti_3AlC_2 MAX powder and (b) 2 g Ti_3AlC_2 MAX pellets (the diameter of each pellet is 14 mm, the thickness of each pellet is 5mm).

Reference

1. J. Halim, K. M. Cook, M. Naguib, P. Eklund, Y. Gogotsi, J. Rosen and M. W. Barsoum, *Applied Surface Science*, 2016, **362**, 406-417.

2. S. Yamamoto, H. Bluhm, K. Andersson, G. Ketteler, H. Ogasawara, M. Salmeron and A. Nilsson, *Journal of Physics: Condensed Matter*, 2008, **20**, 184025.

3. G. Beamson, D. Briggs, *Journal of Chemical Education*, 1993, **70**, A25.

4. U. Diebold and T. E. Madey, *Surface Science Spectra*, 1996, **4**, 227-231.

5. K.-H. Ernst, D. Grman, R. Hauert and E. Holländer*, Surface and Interface Analysis,* 1994, **21**, 691-696.

6. I. Popova, V. Zhukov and J. T. Yates, *Langmuir*, 2000, **16**, 10309-10314.

7. I. Persson, L.-Å. Näslund, J. Halim, M. W. Barsoum, V. Darakchieva, J. Palisaitis, J. Rosen and P. O. Å. Persson, *2D Materials*, 2017, 5, 015002.

8. A. D. Dillon, M. J. Ghidiu, A. L. Krick, J. Griggs, S. J. May, Y. Gogotsi, M. W. Barsoum and A. T. Fafarman, *Advanced Functional Materials*, 2016, **26**, 4162-4168.